Video Article

# Fluorescence Recovery after Merging a Droplet to Measure the Two-dimensional Diffusion of a Phospholipid Monolayer

Dae-Woong Jeong[1], KyuHan Kim[2], Myung Chul Choi[1], Siyoung Q. Choi[2]

[1]Department of Bio and Brain Engineering, KAIST

[2]Information and Electrical Research Institute, KAIST

Correspondence to: Siyoung Q. Choi at sqchoi@kaist.ac.kr

URL: https://www.jove.com/video/53376
DOI: doi:10.3791/53376

Keywords: Bioengineering, Issue 104, FRAM, diffusion, drop coalescence, phospholipid monolayer, FRAP, inter-diffusion, fluid-fluid interfaces

Date Published: 10/15/2015

Citation: Jeong, D.W., Kim, K., Choi, M.C., Choi, S.Q. Fluorescence Recovery after Merging a Droplet to Measure the Two-dimensional Diffusion of a Phospholipid Monolayer. *J. Vis. Exp.* (104), e53376, doi:10.3791/53376 (2015).

## Abstract

We introduce a new method to measure the lateral diffusivity of a surfactant monolayer at the fluid-fluid interface, called fluorescence recovery after merging (FRAM). FRAM adopts the same principles as the fluorescence recovery after photobleaching (FRAP) technique, especially for measuring fluorescence recovery after bleaching a specific area, but FRAM uses a drop coalescence instead of photobleaching dye molecules to induce a chemical potential gradient of dye molecules. Our technique has several advantages over FRAP: it only requires a fluorescence microscope rather than a confocal microscope equipped with high power lasers; it is essentially free from the selection of fluorescence dyes; and it has far more freedom to define the measured diffusion area. Furthermore, FRAM potentially provides a route for studying the mixing or inter-diffusion of two different surfactants, when the monolayers at a surface of droplet and at a flat air/water interface are prepared with different species, independently.

## Video Link

The video component of this article can be found at https://www.jove.com/video/53376/

## Introduction

Phospholipids are major components of cell membranes and the membranes of organelles, and the fluidity of these membrane layers often affects cellular functions by altering the activity of membrane proteins[1–3]. For instance, membrane lipid homeostasis is achieved by regulating membrane fluidity, which is detected by membrane proteins, and an abnormal level of fluidity causes severe diseases, such as hepatic steatosis and cholestasis[4]. In addition, fluidity of a phospholipid monolayer at the air-alveoli fluid interface has important implications in its functions. High fluidity of the lung surfactant phospholipid monolayer facilitates spreading of the layer during inhalation, whereas a low fluidity enables the layer to stay within the alveoli during exhalation[5,6]. It is thus important to estimate the fluidity of the phospholipid layers to understand their roles.

A direct measure of the fluidity is viscosity, and the viscosity of phospholipid layers has been measured by using micron-sized colloids[7], magnetic needles[8,9], and magnetic micro-buttons[6,10,11]. However, these techniques are limited to relatively rigid films, and cannot measure less viscous films. For such cases, diffusivity would be an alternative to quantify fluidity of phospholipid layers. For several decades, a variety of techniques to measure the diffusion properties of phospholipid layers have been developed, such as fluorescence quenching method[12], pulsed field gradient NMR[13], and fluorescence correlation spectroscopy (FCS)[14]. One of the most representative methods is fluorescence recovery after photobleaching (FRAP)[15,16]. Due to the simplicity of the measurement procedure and related theories, several studies on the diffusion properties of phospholipid layers have been performed using FRAP[17–19]. However, FRAP usually requires an expensive confocal microscope setup with a high-power laser.

Here, we present a new technique to measure the lateral diffusion of phospholipid monolayers, termed as fluorescence recovery after merging (FRAM). The key difference between FRAP and FRAM is that the photobleaching step is replaced by the drop coalescence. Merging a droplet covered by non-fluorescence monolayer onto a fluorescently labeled flat monolayer leaves a circular dark stain on a bright flat monolayer, thus setting up the same initial state with the photobleaching step. We then observe the fluorescence recovery in the dark stain with time to measure the lateral diffusivity. This new “bleaching” step by drop coalescence provides significant advantages over FRAP: FRAM only requires a fluorescence microscope rather than an expensive confocal microscope with a high power laser that is necessary for FRAP. In addition, FRAM has a wide selection of fluorescence dyes since it does not involve the photobleaching process. Finally, the two different monolayers, a droplet monolayer and a flat monolayer, can be prepared independently, thus allowing interdiffusion to be measured, while FRAP only measures the self-diffusion of monolayers.

FRAM provides a wide range of diffusion measurements from highly viscous materials to nearly inviscid materials. In principal, FRAM can measure the maximum diffusivity of $10^6$ $\mu m^2$/sec, which is comparable to existing techniques, when the diffusion occurs across the area 100 μm by 100 μm during the time for the drop coalescence process (~ 10 msec). Furthermore, slow diffusion process can be easily measured unless

monolayers are solid. FRAM can be used for any kinds of surface active materials as long as appropriate fluorescently tagged molecules are available.

## Protocol

Caution: Refer to material safety data sheets (MSDS) before use of acetone and chloroform which are carcinogenic.

# 1. Preparation of Phospholipid Monolayer at a Flat Air-water Interface

1. Formation of a phospholipid monolayer
    1. Preparation of a phospholipid solution
        1. Clean a 4 ml vial with a polytetrafluoroethylene coated cap using acetone, ethanol, and deionized water at least three times, and blow nitrogen gas thoroughly into the vial to get rid of water.
        2. Dissolve 1 mg of phospholipid (*e.g.,* dioleoylphosphatidylcholine, DOPC) to 1 ml of chloroform in the vial to obtain 1 mg/ml of concentration. Perform this procedure in a fume hood for safety. Use lower or higher concentrations of phospholipid solution if necessary.
        3. Add dye tagged phospholipids (*e.g.,* Rhodamine dipalmitoylphosphatidylethanolamine, Rhodamine DPPE) with less than 1 mol % of the phospholipid solution, in order to visualize the phospholipid monolayer with a fluorescence microscope. Perform this procedure in a fume hood for safety.
        4. Wrap the vial with a polytetrafluoroethylene tape to prevent solvent evaporation, and store the sample in a freezer at -20 °C.
    2. Deposition of phospholipids onto the air-water interface
        1. Clean a Petri dish (55 mm in diameter and 12 mm in height) with ethanol, and deionized water at least three times.
        2. Fill the Petri dish with 10 ml of deionized water to create an air-water interface.
        3. Spread few microliters of the phospholipid solution with a micro-syringe onto a clean interface to achieve desired surface pressure and wait for at least 30 min to evaporate the solvent completely, prior to doing the experiment.
           Note: A Langmuir trough can be used instead of a Petri dish if precise control of surface pressure is necessary.

2. Surface pressure measurement
    1. Measure the surface pressure of the phospholipid monolayer with a Wilhelmy plate tensiometer. Wait for at least 30 min to get the filter paper wetted enough if filter paper is used as a Wilhelmy plate. The detailed protocol is available in Kuhn *et al.*[20].
    2. Adjust the deposited amount of the phospholipid to control the surface pressure precisely. Add 4 µl of the DOPC solution (1 mg/ml) onto the 30.25 $cm^2$–area of the interface if ~ 5 mN/m of surface pressure is required.
       Note: If the filter paper is not fully wetted, surface pressure changes dramatically during the first 30 min of the experiment due to the weight change of the filter paper.

3. Minimization of the convective flow of the monolayer
    1. Use a cone-shaped apparatus that contains a 3 mm reservoir with two thin channels, connected to a large section of the Petri dish, to suppress the convective flow of the monolayer, which can disturb morphology imaging and surface pressure measurement.
    2. Make sure to match the water levels between the inside and outside of the cone-shape apparatus to ensure that phospholipids move freely over the whole region before depositing phospholipids onto the air-water interface.

# 2. Preparation of Phospholipid Monolayer at the Curved Surface of a Droplet

1. Tapering process of a glass capillary using micropipette puller
    1. Place a glass capillary (o.d. 1 mm, i.d. 0.78 mm, length 100 mm) on a capillary holder of a micropipette puller.
    2. Design a program for pulling the capillaries with appropriate parameter values (Heat: Ramp, Pull: 60, Vel: 70, Delay: 70 and Pressure 200) and pull the capillaries with the designed program according to manufacturer's protocol.
       Note: A capillary end with a few micrometers-diameter is necessary to form a 100 µm-droplet by applying a pressure with ~ 10 kPa. If the tip end of the capillary is too small, much higher pressure, > 600 kPa, is required to obtain the droplet, while it is hard to control the size of the droplets with a too large capillary tip end.

2. Absorption of phospholipids onto the droplet surface
   Note: To form a phospholipid monolayer at the curved interface of a droplet, a phospholipid solution without dye tagged phospholipids is used to obtain an intensity contrast, against the flat monolayer, prepared by procedure 1. In addition, both procedures 2.2.1 and 2.2.2 are allowable here. If precise control of the surface pressure at the droplet surface is necessary, procedure 2.2.2 is highly recommended. However, if not, procedure 2.2.1, which is a much easier way than procedure 2.2.2, is useful.
    1. Coating process of phospholipids at a tip end
        1. Clean a slide glass using acetone, ethanol, and deionized water at least three times.
        2. Place the tapered capillary on a cleaned slide glass, and tilt the capillary to facilitate touching the slide glass with a tip end.
        3. Drop a few droplets of phospholipid solution (1 mg/ml) onto the tip end of a capillary that is adhered to the glass slide using a glass syringe, and wait at least 30 min to evaporate the solvent completely.
           Note: It is highly recommended to adhere the tip end of the capillary to the glass slide during procedure 2.2.1.3 because the perimeter of the tip end is too small to hold the droplet of the phospholipids at the tip end only by capillary force.
    2. Preparation of a vesicle solution
        1. Clean a vial, and remove water from the vial, as introduced in procedure 1.1.1.1.

2. Dry a 2 ml volume of phospholipid solution (1 mg/ml) by applying nitrogen gas gently, and desiccate the vial for 1 hr at RT to eliminate any remaining solvent. Perform this procedure in a fume hood for safety.
3. Add 2 ml of deionized water into the vial containing dried lipids, and incubate the vial in an oven at 60 °C for 1 hr.
4. Shake the vial several times, and sonicate (HF-frequency: Up to 40 kHz, Power: 370 W) for 30 min to obtain vesicles.
5. Perform extrusion and freeze-thaw processes to obtain monodisperse unilamellar vesicles. The detailed protocol for preparing vesicles is described in Mayer *et al.*[21].
   Note: Surface pressure of the droplet interface is controlled precisely by adjusting the waiting time after formation of the droplet that contains monodisperse unilamellar vesicles. Using a pendant drop method[22], it is necessary to measure the change of surface pressure according to time, prior to doing the experiment.

3. Formation of a droplet that contains a phospholipid monolayer at the curved surface
   1. Fill in the tapered capillary with 10 µl of deionized water from procedure 2.2.1. Alternatively, use 10 µl of the vesicle solution from procedure 2.2.2.
   2. Connect the capillary to an automated micro-injector to provide the pressure to form the droplet.
   3. Mount the capillary that is connected to a micro-injector to a micromanipulator to control the position of the capillary precisely.
   4. Prepare a bright field microscope (Microscope 1, objective lens: 10X NA 0.3) for imaging the lateral view of the capillary with a CCD camera. Microscope 1 thus enables to observe the precise position of the droplet along the z-axis and estimate the size of the droplet.
   5. Move the tip end to a position where the lateral view of the tip end is well visualized by Microscope 1 using a micromanipulator, and apply a variable pressure (~ 100 hPa) with the tip end of the capillary, until an appropriate size (~100 µm in diameter) of droplet is formed.
      Note: It is recommended that automated micro-injector and micromanipulator be used, if fine control of the droplet size and location of the droplet is necessary. It is also possible to use manual ones.

## 3. Imaging Fluorescence Recovery after Droplet Merging

Note: The fundamental principles of this protocol are identical to those of the FRAP technique, except for the drop coalescence process. The detailed protocol and related theories of FRAP are available in A. Lopez *et al.*[15] and D. Axelrod *et al.*[16].

1. Monitoring and controlling the location of the droplet
   1. Prepare an inverted microscope set (Microscope 2, objective lens: 10X NA 0.3, tube lens: focal length 17 cm) that enables both a fluorescence microscope with a proper filter set for Rhodamine-DPPEs (excitation at 560 nm, emission at 583 nm) and a bright field microscope. Use a CCD camera here for visualizing the top views of the droplet with a fluorescence microscope mode and a bright-field microscope mode.
   2. Move the droplet coated with a phospholipid to a flat air-water interface along the z-axis, but do not merge the droplet yet, using the micromanipulator. Use Microscope 1 to visualize the lateral view of the droplet.
   3. Locate the droplet at the center of the top view of the flat monolayer, using the micromanipulator. Use the bright-field microscope mode of Microscope 2 to visualize top view of flat monolayer.

2. Merging the droplet onto the flat air-water interface
   1. Move the droplet further toward the flat interface until the droplet merges onto the interface, using the micromanipulator. If the merging process is done successfully, a dark region with a circular shape that is surrounded by a white background, is observed using the fluorescence mode of Microscope 2.
   2. Record the series of fluorescent images according to time after merging the droplet, using the fluorescence mode of Microscope 2. Use a faster frame rate than the diffusion time scale of the monolayer here. In DOPC monolayer, it takes a few minutes to diffuse into the 200 µm-dark area completely.

## 4. Determining the Diffusion Coefficient by Image Analysis

Note: To determine the diffusion coefficient from a series of images, customized program for image analysis is built as described below. A detailed source code of this program is available in JoVE website.

1. Detection of a circular region of interest
   1. Detection of the center of the region of interest
      1. Obtain a series of fluorescent images that have been recorded during a recovery process which contains a circular dark area and a white background, and set the first image of the series as a reference image. Here, $R_D$ is the radius of the dark area in a reference image.
      2. Convolute the reference image with a white circle whose intensity is uniform over a whole region. Use embedded function named ‘conv2’ for convolution as shown in the source code of the customized program line 124. Here, the radius of the white circle is slightly smaller than $R_D$.
      3. Find a position that indicates a minimum value in the convolution calculation, and set this position as the center of the region of interest in the reference image.

   2. Determining a radius of the region of interest
      1. Convolute the reference image with a white circle that contains a center position, determined by a procedure 4.1 and uniform intensity over a whole region. Here, $R_S$ is the radius of the white circle. Use iteration such as ‘for’ or ‘while’ with equation of a circle to make the white circle as shown in the source code of the customized program line 102 to 109.

2. Convolute the reference image with another white circle which has a slightly larger radius (5%–10%), $R_L$, than $R_S$. Use same method with procedure 4.1.2.1 to make the circle as shown in the source code of the customized program line 113 to 120.
3. Obtain the difference in value between the two convolution calculations of 4.1.2.1 and 4.1.2.2.
4. Repeat the above procedures from $R_S = R_D/2$ to $R_S = 2R_D$, by increasing both the $R_S$ and $R_L$ with a pixel level. Make an iteration that contains whole source codes from procedure 4.1.2.1 to 4.1.2.3 to repeat.
5. Find the radius of $R_S$ that indicates the maximum difference in value between the two convolution calculations. Use embedded function named 'max' to find the radius indicates the maximum difference in value as shown in the source code of the customized program line 148 to 149. This $R_S$ thus indicates the radius of the dark area in the reference image.

2. Calculation of a fractional intensity
   1. Set a circle that contains a center position and a radius, determined by procedure 4.1 as a region of interest.
   2. Calculate the average intensities of the region of interest in a series of fluorescence images according to time. Convolute each frame with region of interest and divide it by area of region of interest to calculate the average intensity. The details are available in the source code of the customized program which is available in JoVE website.
   3. Calculate a fractional intensity, defined as the equation below, where F(t) is the average intensity in the circle that is a region of interest according to time, $F_i$ is the initial intensity in the circle, and $F_o$ is the intensity of a white background.
      $f(t) = (F(t) - F_i)/(F_o - F_i)$ (Equation 1).

3. Fitting the fractional intensity to FRAP theory
   1. Fit the fractional intensity with the equation below, where τ is a characteristic diffusion time and $I_0$, $I_1$ are modified Bessel functions, using a fitting program, and obtain τ
      $$f(t) = Ce^{-2\tau/t}\left[I_0\left(\frac{2\tau}{t}\right) + I_1\left(\frac{2\tau}{t}\right)\right]$$ (Equation 2).
   2. Obtain a diffusion coefficient based on the relation, $\tau = a^2/4D$, where D is the diffusion coefficient and a is the radius of the dark area. Note: During the fitting process, it is possible to shift the fractional intensity profile along a time axis when the recovery process has already started, before recording the images.

## Representative Results

A series of fluorescence images were obtained with time during the recovery process after merging a droplet coated with a DOPC monolayer onto a flat DOPC monolayer, as listed in **Figure 1**. The DOPC monolayer at the flat air-water interface was doped with low amounts of Rhodamine-DPPE, and this thus made it possible to visualize a background with a bright color and a dark region newly added to the flat interface. There, a recovery process was observed at 23 mN/m of fixed surface pressure. A fit of equation 1 to the change of fractional intensity according to time is shown in **Figure 2**. The $R^2$ value of this fit is 0.999, and this fit still works well even at lower or higher surface pressures. The diffusion coefficient of the DOPC monolayer obtained from this fit was 27.54 $\mu m^2$/sec at 23 mN/m of surface pressure.

For further validation of the FRAM, diffusion coefficients of the DOPC and dipalmitoylphosphatidylcholine (DPPC) monolayers were measured according to surface pressure. As shown in **Figure 3**, FRAM captures the rapid decrease of diffusion coefficient of the DPPC monolayer at ~ 9 mN/m of surface pressure, where a LC (liquid condensed) – LE (liquid expanded) phase transition occurs[10], and the values of diffusion coefficients are also agreed well with the previously measurements by Peters *et al.*[19]. In addition, an exponential decay of the diffusion coefficient with the surface pressure was observed in the DOPC monolayer, and this tendency is almost identical with the one measured by Caruso *et al.*[12].

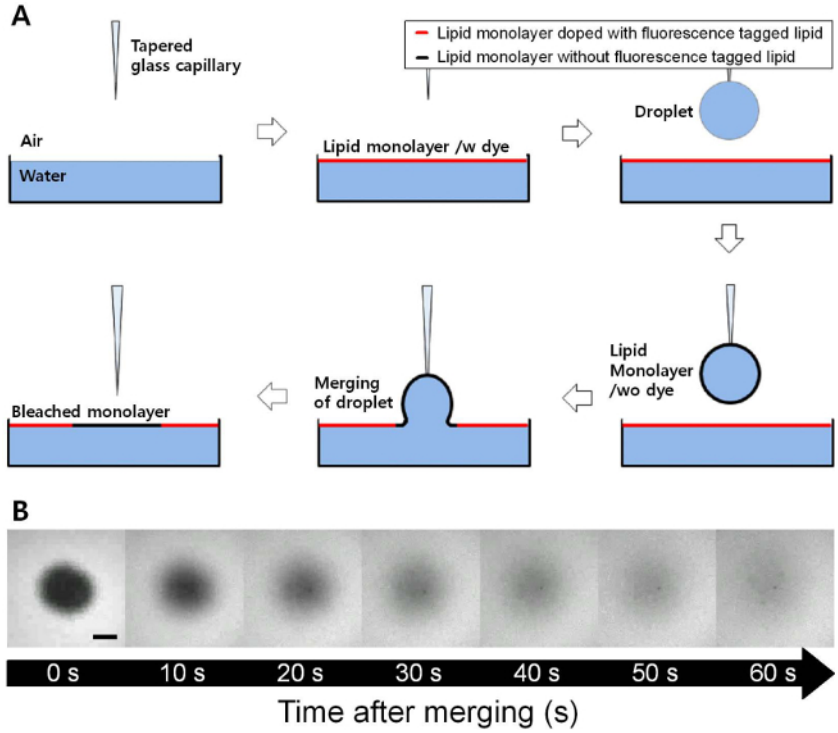


**Figure 1.** (**A**) Schematic illustration of the FRAM (fluorescence recovery after merging) technique. As the lipid monolayer coated droplet is merged to flat air-water interface, the lipid monolayer without fluorescence tagged lipid is inserted into flat fluorescent lipid monolayer. (**B**) Fluorescence microscope images with time during the recovery process of a DOPC monolayer at 23 mN/m of surface pressure (scale bar = 100 μm). The dark region of the DOPC monolayer is fully recovered by the diffusion process within several minutes. Please click here to view a larger version of this figure.

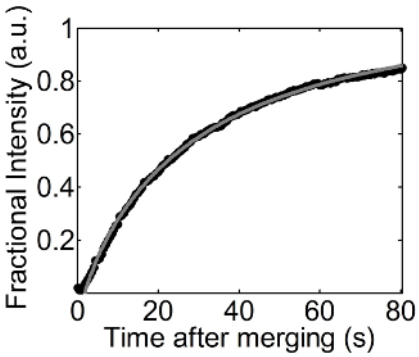


**Figure 2.** Fractional intensity vs. time. Black circles and the gray dotted line indicate the values of fractional intensities obtained from image analysis (procedures 4.1 and 4.2) and the fit of equation 1 to the fractional intensities with time, shown in procedure 4.3, respectively. Please click here to view a larger version of this figure.

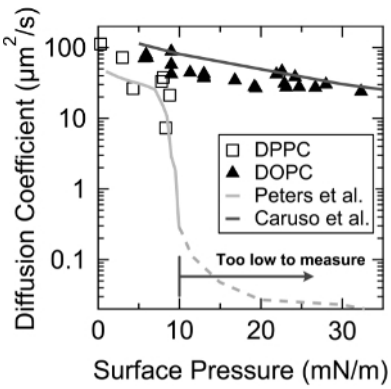


**Figure 3.** Diffusion coefficients of DOPC (triangle) and DPPC (empty square) monolayers as a function of surface pressure. The lines with the bright gray color and with the dark gray color indicate the values of the diffusion coefficient previously reported by Peters *et al.* and Caruso *et al.*, respectively. This figure has been modified from Jeong *et al.*[23]. Reprinted with permission from Jeong *et al*. *Langmuir*. **30**(48), 14369-14374. Copyright 2014 American Chemical Society. Please click here to view a larger version of this figure.

## Discussion

FRAM shares a lot of fundamental principles with FRAP, especially for measuring fluorescence recovery after bleaching a specific area, but FRAM uses a process of merging a droplet onto the flat interface to form a bleached area, instead of applying an intensive light. The merging process is thus most important step in FRAM, and especially, the shape of the dark stain at the flat monolayer after merging a droplet determines the accuracy of the diffusivity measurement. Specifically, based on a current method, we only set the circle with a radius R as a region of interest to calculate the average intensity of the dark stain, shown in procedure 4, and if there is a too much deviation from the circular shape, this would disturb the precise measurement of a diffusion coefficient. Therefore, it is necessary to obtain a circular shaped dark region, but, noncircular shapes are formed occasionally due to several reasons. First, if there exists a convective flow in the Petri dish, the shape of the dark area becomes elongated along the direction of flow. As mentioned in procedure 1.3, a cone-shape apparatus helps to suppress the convective flow, and this elongation would be minimized. Second, if the tip end of the capillary touches the flat interface during a merging process, the dark area is formed with a variety of shapes since the capillary end interrupts the merging process. By obtaining a droplet that is only hanging from the very end of the capillary, this interruption can be prevented. In particular, a hydrophobic treatment of the capillary helps the droplet to sit at the very end of the capillary. Therefore, above trouble shootings and modifications enable us to measure diffusion properties more precisely.

This well troubleshot process thus allows FRAM to have several significant advantages over FRAP. First, FRAM requires simpler equipment compared to FRAP. For FRAM, it is sufficient to use a simple fluorescence microscope, instead of an expensive confocal microscope with a high power laser whose wavelength must match with the absorption spectrum of the dye. In addition, it is necessary to use additional apparatus to adjust the size to the bleached area in the FRAP, while the FRAM controls the size of the area easily by adjusting the size of the droplet, or the surface pressure at the droplet surface. Second, it is possible to use various species of dyes in FRAM. FRAP only uses dye molecules whose bleaching process is much faster than the diffusion process. If the diffusion of the dyes occurs during the bleaching process, it is hard to estimate the diffusion property accurately. The FRAM, however, does not require a process for bleaching dyes and this thus enables the use of various types of dyes in the fluorescence imaging. In addition, the FRAP requires additional high power lasers and filter sets to change the dye species, while it is only necessary to replace the filter sets in the FRAM. Finally, since the monolayers at the droplet surface and the flat interface can be formed independently, thus enabling the study of inter-diffusion or mixing between two different lipid monolayers by merging A-type monolayer to B-type monolayer, while the FRAP only measures the self-diffusion of a monolayer.

Despite these advantages, the process of merging a droplet onto a flat air-water interface can potentially limit this technique due to several issues that might be of concern, such as a surface pressure mismatch between the two monolayers, the time scale of the merging process, and an increase in the surface pressure of the flat monolayer after merging droplets. These issues, however, do not affect the diffusion measurement significantly for the following reasons. First, even though the surface pressures at the two different monolayers are quite different, an equilibration process is completed at a very early stage during the recovery process. For example, if the surface pressure of the monolayer at the droplet surface is higher than that of the monolayer at the flat air-water interface, the dark area expands until the surface pressure equilibrates. Since this process is completed within 10 msec, the surface pressure will be equilibrated before it affects the diffusion process significantly. Second, if the time scale of the merging process is fast enough, it does not limit the diffusion measurement at all. Fortunately, a typical merging process is also completed within 10 msec. Finally, even multiple merging of the droplets onto the flat interface do not increase the surface pressure since the surface area of the trough is far larger than the surface area of the droplet. According to the sizes of the trough and the droplets, described in the protocol, the area per molecule increases less than 0.015% by merging a droplet. Accordingly, the increase of surface pressure due to the change of area per molecule is less than 0.1%, which is negligible because it is much smaller than the typical error in surface pressure, as measured by Wilhelmy plate tensiometer.

In summary, we introduced a new method to measure the lateral diffusion property of a phospholipid monolayer by merging a droplet monolayer onto the flat interface. This technique requires relatively simple equipment and also enables the use of various sorts of dye species. The FRAM is thus potentially applicable for diffusion measurement of any surface active agents, including phospholipids, block copolymers, proteins and even nanoparticles at a fluid-fluid interface. Furthermore, we expect that the FRAM provides a new way to study the inter-diffusion or mixing between two different surface active agents.

## Disclosures

The authors declare no competing financial interest.

## Acknowledgements

This work is supported by the KAIST-funded K-Valley RED&B Project for 2014 and the Basic Science Research Program through the National Research Foundation of Korea (NRF- 2012R1A6A3A040395, NRF-2013R1A1A2057708, NRF- 2012R1A1A1011023).

## References

1. Van Meer, G., Voelker, D. R., & Feigenson, G. W. Membrane lipids: where they are and how they behave. *Nat. Rev. Mol. Cell Biol.* **9** (2), 112-124, doi: 10.1038/nrm2330 (2008).
2. Christon, R., Even, V., Daveloose, D., Léger, C. L., & Viret, J. Modification of fluidity and lipid—protein relationships in pig intestinal brush-border membrane by dietary essential fatty acid deficiency. *Biochim. Biophys. Acta - Biomembr.* **980** (1), 77-84, doi: 10.1016/0005-2736(89)90202-2 (1989).
3. Stubbs, C. D., & Smith, a. D. The modification of mammalian membrane polyunsaturated fatty acid composition in relation to membrane fluidity and function. *Biochim. Biophys. Acta - Rev. Biomembr.* **779** (1), 89-137, doi: 10.1016/0304-4157(84)90005-4 (1984).
4. Holthuis, J. C. M., & Menon, A. K. Lipid landscapes and pipelines in membrane homeostasis. *Nature.* **510**(7503), 48-57, doi: 10.1038/nature13474 (2014).
5. Alonso, C., Waring, A., & Zasadzinski, J. A. Keeping lung surfactant where it belongs: protein regulation of two-dimensional viscosity. *Biophys. J.* **89** (1), 266-273, doi: 10.1529/biophysj.104.052092 (2005).
6. Kim, K., Choi, S. Q., Zell, Z. a, Squires, T. M., & Zasadzinski, J. a. Effect of cholesterol nanodomains on monolayer morphology and dynamics. *Proc. Natl. Acad. Sci. (U. S. A.).* **110** (33), E3054-60, doi: 10.1073/pnas.1303304110 (2013).
7. Hormel, T. T., Kurihara, S. Q., Brennan, M. K., Wozniak, M. C., & Parthasarathy, R. Measuring Lipid Membrane Viscosity Using Rotational and Translational Probe Diffusion. *Phys. Rev. Letters.* **112** (18), 188101, doi: 10.1103/PhysRevLett.112.188101 (2014).
8. Ding, J., Warriner, H. E., Zasadzinski, J. a., & Schwartz, D. K. Magnetic needle viscometer for Langmuir monolayers. *Langmuir.* **18** (13), 2800-2806, doi: 10.1021/la015589+ (2002).
9. Dhar, P., Cao, Y., Fischer, T. M., & Zasadzinski, J. a. Active interfacial shear microrheology of aging protein films. *Phys. Rev. Letters.* **104** (1), 1-4, doi: 10.1103/PhysRevLett.104.016001 (2010).
10. Kim, K., Choi, S. Q., Zasadzinski, J. a., & Squires, T. M. Interfacial microrheology of DPPC monolayers at the air-water interface. *Soft Matter.* **7** (17), 7782-7789, doi: 10.1039/c1sm05383c (2011).
11. Choi, S. Q., Steltenkamp, S., Zasadzinski, J. a & Squires, T. M. Active microrheology and simultaneous visualization of sheared phospholipid monolayers. *Nature Commun.* **2** (5), 312, doi: 10.1038/ncomms1321 (2011).
12. Caruso, F. *et al.* Determination of lateral diffusion coefficients in air-water monolayers by fluorescence quenching measurements. *J. Am. Chem. Soc.* **113** (16), 4838-4843, doi: 10.1021/ja00013a019 (1991).
13. Filippov, A., Orädd, G., & Lindblom, G. The effect of cholesterol on the lateral diffusion of phospholipids in oriented bilayers. *Biophys. J.* **84** (5), 3079-3086, doi: 10.1016/S0006-3495(03)70033-2 (2003).
14. Schwille, P., Korlach, J., & Webb, W. W. Fluorescence correlation spectroscopy with single-molecule sensitivity on cell and model membranes. *Cytometry.* **36** (3), 176-182, doi: 10.1002/(SICI)1097-0320(19990701)36:3<176::AID-CYTO5>3.0.CO;2-F (1999).
15. Lopez, A., Dupou, L., Altibelli, A., Trotard, J., & Tocanne, J. F. Fluorescence recovery after photobleaching (FRAP) experiments under conditions of uniform disk illumination. Critical comparison of analytical solutions, and a new mathematical method for calculation of diffusion coefficient D. *Biophys. J.* **53** (6), 963-970, doi: 10.1016/S0006-3495(88)83177-1 (1988).
16. Axelrod, D., Koppel, D. E., Schlessinger, J., Elson, E., & Webb, W. W. Mobility measurement by analysis of fluorescence photobleaching recovery kinetics. *Biophys. J.* . **16** (9), 1055-1069, doi: 10.1016/S0006-3495(76)85755-4 (1976).
17. Vaz, W. L., Clegg, R. M., & Hallmann, D. Translational diffusion of lipids in liquid crystalline phase phosphatidylcholine multibilayers. A comparison of experiment with theory. *Biochemistry.* **24** (3), 781-786, doi: 10.1021/bi00324a037 (1985).
18. Wu, E. S., Jacobson, K., & Papahadjopoulos, D. Lateral diffusion in phospholipid multibilayers measured by fluorescence recovery after photobleaching. *Biochemistry.* **16** (17), 3836-3841, doi: 10.1016/S0006-3495(88)83177-1 (1977).
19. Peters, R., & Beck, K. Translational diffusion in phospholipid monolayers measured by fluorescence microphotolysis. *Proc. Natl. Acad. Sci. (U. S. A.).* **80** (23), 7183-7187 (1983).
20. Kuhn, H., Mobius, D & Bucher, H. *Physical Methods of Chemistry.* Crawley, J.N., et al., eds., Vol. 1, Part 3B, 651-653 (1972).
21. Mayer, L. D., Hope, M. J., & Cullis, P. R. Vesicles of variable sizes produced by a rapid extrusion procedure. *Biochim. Biophys. Acta - Biomembr.* **858** (1), 161-168, doi: 10.1016/0005-2736(86)90302-0 (1986).
22. Rotenberg, Y., Boruvka, L., & Neumann, A. . Determination of surface tension and contact angle from the shapes of axisymmetric fluid interfaces. *J. Colloid Interface Sci.* **93** (5), 169-183, 10.1016/0021-9797(83)90396-X (1983).
23. Jeong, D.-W., Kim, K., Lee, S., Choi, M. C., & Choi, S. Q. Fluorescence recovery after merging a surfactant-covered droplet: a novel technique to measure the diffusion of phospholipid monolayers at fluid/fluid interfaces. *Langmuir.* **30** (48), 14369-14374, doi: 10.1021/la503219n (2014).